Supplementary Materials to "Multi-Game Decision Transformers"

A Implementation Details

A.1 Transformer network architecture

The input consists of a sequence of observations, returns, actions and rewards. Observations are images in the format $B \times T \times W \times H \times C$. We use 84×84 grayscale images (*i.e.*, $W = 84, H = 84, C = 1$). Similar to ViT [6], we extract M non-overlapping image patches, perform a linear projection and then rasterise them into d_{model}-dimensional 1D tokens. We define each patch to be 14×14 pixels (*i.e.*, $M = 6 \times 6 = 36$). A learned positional embedding is added to each of the patch tokens $\mathbf{o}_1, ..., \mathbf{o}_M$ to retain positional information as in ViT. As described in Section 3.2, returns are discretized into 120 buckets in $\{-20, ..., 100\}$, and rewards are converted to ternary quantities $\{-1, 0, +1\}$.

For the whole sequence $\langle ..., \mathbf{o}_1^t, ..., \mathbf{o}_M^t, \hat{R}^t, a^t, r^t, ... \rangle$, we learn another positional embedding at each position and add to each token embedding. We experimented with rotary position embedding [16], but did not find a significant benefit from them in our setting. On top of the token embeddings, our transformer models use a standard transformer decoder architecture.

A standard transformer implementation for sequence modeling would employ a sequential causal attention masking to prevent positions from attending to subsequent positions [17]. However, for the sequence $\langle ..., \mathbf{o}_1^t, ..., \mathbf{o}_M^t, \hat{R}^t, a^t, r^t, ... \rangle$ that we consider, we do not want to prevent the position corresponding to observation token $\mathbf{o}_m^t$ from accessing subsequent observation tokens $\{\mathbf{o}_{m'}^t : m' > m\}$ within the same timestep, since there is no clear sequential causal relation between image patches. Therefore, we change the sequential causal masking to allow observation tokens within the same timestep to access each other, but not subsequent positions after $\mathbf{o}_M^t$, *i.e.* $\hat{R}^t, a^t, r^t, \mathbf{o}_1^{t+1}, ..., \mathbf{o}_M^{t+1}, ...$

Table 1 summarizes the transformer configurations we use for each model size. We train these models on an internal cluster, each with 64 TPUv4. Due to prohibitively long training times, we only evaluated one training seed.

Model	Layers	Hidden size D (d_{model})	Heads	Params	Training Time on 64 TPUv4
DT-10M	4	512	8	10M	1 day
DT-40M	6	768	12	40M	2 days
DT-200M	10	1280	20	200M	8 days

Table 1: Multi-Game Decision Transformer Variants

A.2 Fine-tuning protocol for Atari games

In the fine-tuning experiments, we reserved five games (Alien, MsPacman, Pong, Space Invaders and Star Gunner) to be used only for fine-tuning. These games were selected due to their varied gameplay characteristics. Each game was fine-tuned separately to measure the model's transfer performance for a fixed game. We use 1% of the original dataset (corresponding to roughly $500\,000$ transitions) to specifically test fine-tuning in low-data regimes.

A.3 Action and return sampling during in-game evaluation

We sample actions from the model with a temperature of 1. Inspired by Nucleus sampling (Holtzman et al. [10]), we only sample from the top 85th percentile action logits for all Decision Transformer models and Behavioral Cloning models (this parameter was selected to give highest performance for

Submitted to 36th Conference on Neural Information Processing Systems (NeurIPS 2022). Do not distribute.

both models). While we train the model to predict actions for all timesteps in the sequence, during in-game evaluation, we execute the last predicted action in the sequence (conditioned on all past observations, and past generated actions, rewards, and target returns).

To generate target returns as discussed in Section 3.4, we sample them from the model with the temperature of 1 and the top 85th percentile logits. We use $\kappa = 10$ in all our experiments. To avoid storing the history of previously generated target returns (which may be difficult to incorporate into some RL frameworks), we experimented with autoregressively regenerating all target returns in the sequence, and found that to work well without requiring any special recurrent state maintenance outside of the model.

As an alternative way to generate expert-but-likely returns, we also experimented with simply generating N return samples from the model according to log-probability $\log P_\theta(R^t|...)$, and picking the highest one. We then generate the action conditioned on this largest picked return as before. This avoids needing the hyperparameter κ. In this setting, we found $N = 128$, inverse temperature of 0.75 for return sampling, no percentile cutoff for return sampling, and sampling from the top 50th percentile action logits with a temperature of 1 to work similarly well.

A.4 Evaluation protocol and Atari environment details

Our environment is the Atari 2600 Gym environment with pre-processing performed as in Agarwal et al. [1]. Our Atari observations are 84×84 grayscale images. We compress observation images to jpeg in the dataset (to keep dataset size small) and during in-game evaluation. All games use the same shared set of 18 discrete actions. For all methods, each game score is calculated by averaging over 16 model rollout episode trials. To reduce inter-trial variability, we do not use sticky actions during evaluation.

A.5 Data augmentation

All models were trained with data augmentations. We investigate training with the following augmentation methods: random cropping, random channel permutation, random pixel permutation, horizontal flip, vertical flip, and random rotations. We found random cropping and random rotations to work the best. (In our random cropping implementation, images of size 84×84 are padded on each side with 4 zero-value pixels, and then randomly cropped to 84×84.) In general, we aim to expand the domain of problems solved during training to similar kinds that we hope to generalize to by encoding useful inductive biases. We maintain the same random augmentation parameters for each window sequence. We apply data augmentation in both pre-training and fine-tuning.

B Baseline Implementation Details

BC Our BC model is effectively the same as our DT model but removing the return token $\hat{R}^t$ from the training sequence:

$$x \;=\; \langle ..., \mathbf{o}_1^t, ..., \mathbf{o}_M^t, a^t, r^t, ... \rangle$$

Instead of predicting a return token (distribution) given observation tokens $\mathbf{o}_1^t, ..., \mathbf{o}_M^t$ and the previous part of the sequence, we directly predict an action token (distribution), which also means that we remove return conditioning for the BC model. During evaluation, we sample actions with a temperature of 1, and sample from the top 85th percentile logits (as discussed in Appendix A.3). All other implementation details and configurations are identical to DT.

C51 DQN For single-game experiments, our implementation and training followed the details in [3] except for using multi-step learning with $n = 4$. For multi-game experiments we trained using the details provided in the main text; we ran the algorithm for 15M gradient steps ($\approx$ 4B environment steps $\approx$ 16B Atari frames).

CQL For CQL we use the same optimizer and learning rate as for C51 DQN. We use a per-replica batch size of 32 and run for 1M gradient steps on a TPU pod with 32 cores, yielding a global batch size of 256. During finetuning for each game, we copy the entire Q-network trained with CQL, and apply an additional 100k gradient steps of batch size 32 on a single CPU, where each batch is sampled

exclusively from the offline dataset of the finetuned game. We also experimented with smaller learning rates (0.00003 instead of the default 0.00025) but found the results largely unchanged. We also tried using offline C51 and double DQN as opposed to CQL, and found performance to be worse.

CPC For the CPC baseline [13], we apply a contrastive loss between $\phi(o_t), \phi(o_{t+1})$ using the objective function

$$- \phi(o_{t+1})^\top W \phi(o_t) + \log \mathbb{E}_{\tilde{s} \sim \rho}[\exp\{\phi(\tilde{o})^\top W \phi(o_t)\}], \tag{1}$$

where W is a trainable matrix and ρ is a non-trainable prior distribution; for mini-batch training we set ρ to be the distribution of states in the mini-batch. The state representations $\phi(o)$ is parametrized by CNNs followed by two MLP layers with 512 units each interleaved with ReLU activation. For the CNN architecture, we used the C51 implementation with an Impala neural network architecture of three blocks using 16, 32, and 32 channels respectively, and trained with a batch size of 256 and learning rate of 0.00025 both during pretraining and downstream BC adaptation. We conduct representation learning for a total of 1M gradient steps, and finetune on 1% data for 100k steps every 50k steps of representation learning and report the best finetuning results.

BERT and ACL Our BERT and ACL baselines are based on the representation learning objectives described in [18]. For the BERT [5] state representation learning baseline, we (1) take a sub-trajectory $o_{t:t+k}, a_{t:t+k}, r_{t:t+k}$ from the dataset (without special tokenization as in DT), (2) randomly mask a subset of these, (3) pass the masked sequence into a transformer, and then (4) for each masked input state o_{t+i}, apply a contrastive loss between its representation $\phi(o_{t+i})$ and the transformer output $\mathrm{Transformer}[i]$ at the corresponding sequence position:

$$- \phi(o_{t+i})^\top W \,\mathrm{Transformer}[i] + \log \mathbb{E}_{\tilde{o} \sim \rho}[\exp\{\phi(\tilde{o})^\top W \,\mathrm{Transformer}[i]\}], \tag{2}$$

where ρ is the distribution over states in the mini-batch. For attentive contrastive learning (ACL) [18], we apply an additional action prediction loss to the output of BERT at the sequence positions of the action inputs.

To parameterize ϕ, we use the same CNN architecture as in CPC, while the transformer is parameterized by two self-attention layers with 4 attention heads of 256 units each and feed-forward dimension 512. The transformer does not apply any additional directional masking to its inputs. We used $k = 16$.

Pretraining and finetuning is analogous to CPC. Namely, when finetuning we take the pretrained representation ϕ and use a BC objective for learning a neural network (two MLP layers with 512 units each) policy on top of this representation.

C Comparisons between methods based on Inter-Quartile Mean Scores

We used median human-normalized scores to aggregate performance over individual games in Figure 1 and Figure 5, following [1]. It was discussed in [2] that the median has high variability, and in the most extreme case, the median is unaffected by zero performance on nearly half of the tasks. Therefore, we follow the evaluation practice proposed in [2] to also compute Inter-Quartile Mean (IQM) across all games as another aggregate metric. We present Figure 9 as the IQM version of Figure 1, and Figure 10 as the IQM version of Figure 5. We can observe that our conclusions on the benefits of Multi-Game Decision Transformers do not change. Furthermore, in the following sections in the Appendix, we report aggregate performance in both median and IQM scores.

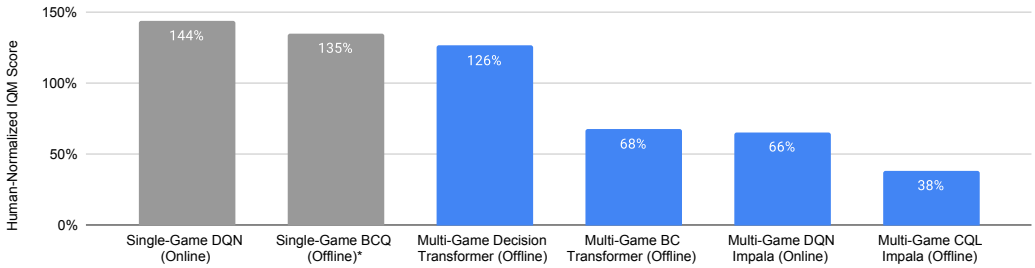

Figure 9: Aggregates of human-normalized scores across 41 Atari games based on Inter-Quartile Mean (IQM). Grey bars are single-game specialist models while blue are generalists. Single-game BCQ [8] results are from Gulcehre et al. [9]. Multi-game models are all trained on a dataset [1] with inter-quartile mean human-normalized score of 101%, which Multi-Game DT notably exceeds.

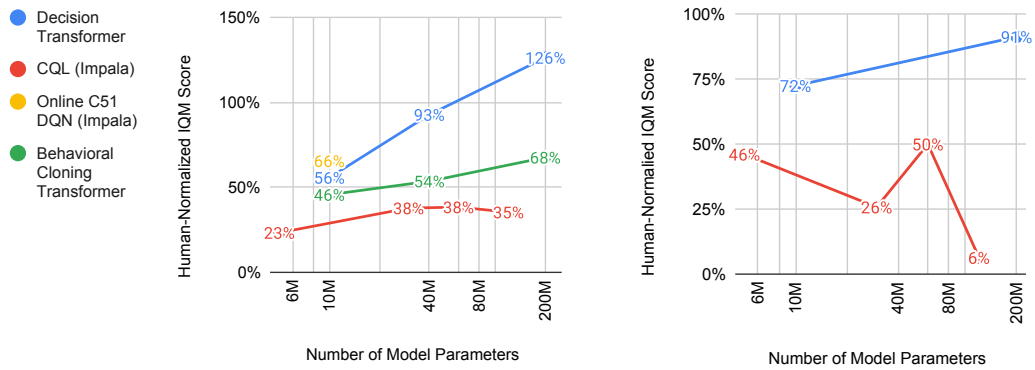

(a) Scaling of IQM scores for all training games with different model sizes and architectures.

(b) Scaling of IQM scores for all novel games after fine-tuning DT and CQL.

Figure 10: How model performance (IQM scores) scales with model size, on training set games and novel games.

D Learning Exclusively from Expert Data

Our DT and baseline models all use the full Atari datasets for training, which include large amounts of sub-optimal, non-expert behavior. We believe that learning from large, diverse datasets in this way helps learning and improves performance. To verify this hypothesis, we experiment with training our DT model and baseline BC model on a filtered version of the training data [1], for which we preserve only the top 10% of episodes from each game according to computed episodic return. We plot return histograms in Figure 11. We use this expert dataset to train our multi-game decision transformer (DT-40M) and the transformer-based behavioral cloning model (BC-40M). Figure 12 and Figure 13 compare these models trained on expert data and our DT-40M trained on all data.

We observe that: (1) Training only on expert data improves behavioral cloning; (2) Training on full data, including expert and non-expert data, improves Decision Transformer; (3) Decision Transformer with full data outperforms behavioral cloning trained on expert data.

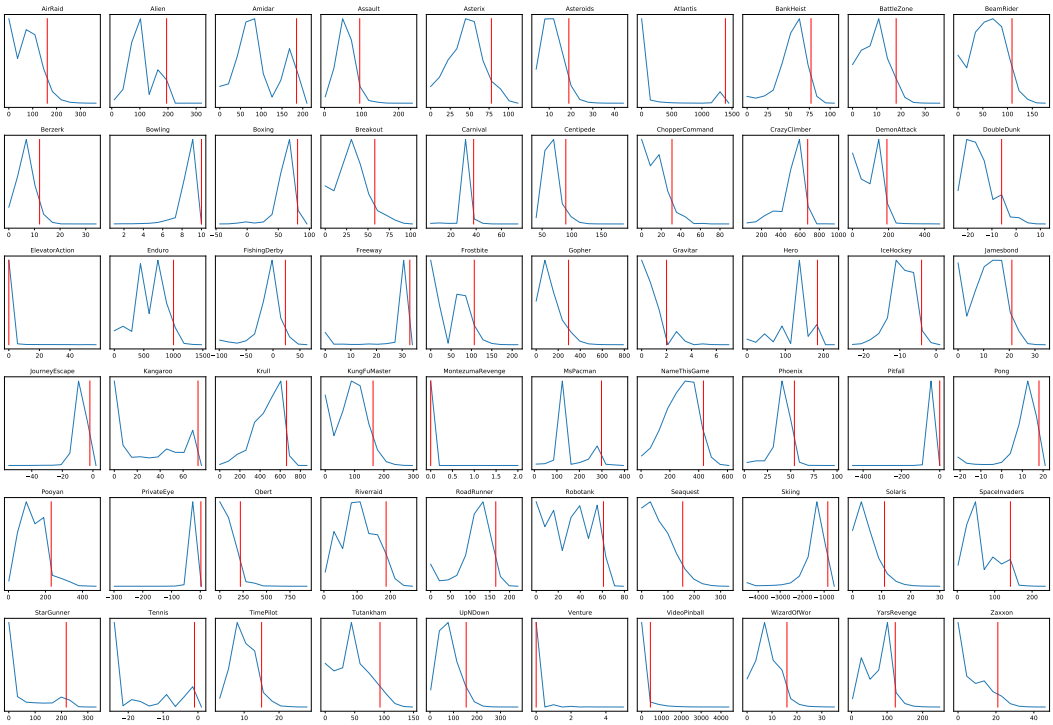

Figure 11: Histograms of rollout performance from [1] used to generate the expert dataset, with (unnormalized) score-density on the vertical axis, and game score (rewards are clipped) on the horizontal axis. We indicate the 90th percentile performance cutoff with a red vertical line for each game. Rollouts that exceeded this score threshold were included in the expert dataset.

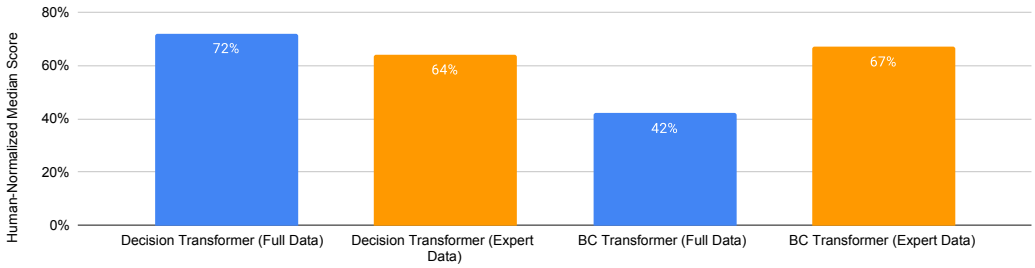

Figure 12: Comparison of 40M transformer models trained on full data and only expert data, in terms of median human-normalized scores.

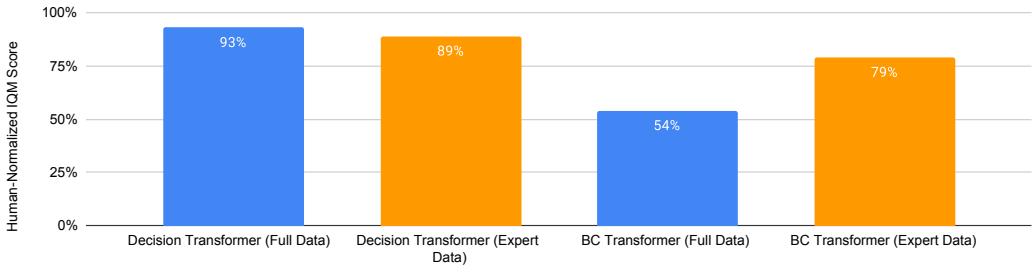

Figure 13: Comparison of 40M transformer models trained on full data and only expert data, in terms of IQM of human-normalized scores.

E Comparisons between transformers and convolution networks

Decision Transformer is an Upside-Down RL (UDRL) [14, 15] implementation that uses the transformer architecture and considers RL as a sequence modeling problem. To understand the benefit of the transformer architecture, we compare to an UDRL implementation that uses feed-forward, convolutional Impala networks [7]. Specifically, we use the same return, action, and reward tokenizers as in DT, and only replace the observation (four consecutive Atari frames stacked together) encoding to use the Impala architecture. Similar to what we do for CQL, we also experiment with different sizes of the Impala architecture by varying the number of blocks and channels in each block of the Impala network: the number of blocks and channels is one of $(5 \text{ blocks}, 128 \text{ channels}) \approx 5\text{M params}$, $(10 \text{ blocks}, 256 \text{ channels}) \approx 30\text{M params}$, $(5 \text{ blocks}, 512 \text{ channels}) \approx 60\text{M params}$. We use a $(768, 768)$ 2-layer fully-connected head to predict the next return token from observation embedding; another $(768, 768)$ head to predict the next action token from a concatenation of observation embedding and return token embedding; another $(768, 768)$ head to predict the next reward token from a concatenation of observation embedding, return token embedding, and action token embedding.

The input to the model is slightly different from what we have for DT: Instead of considering a T-timestep sub-trajectory ($T = 4$) where each timestep contains $\mathbf{o}^t, R^t, a^t, r^t$, we stack T image frames (as common in [12]), and only consider R^t, a^t, r^t from the last timestep. All other design choices and evaluation protocols are the same as DT.

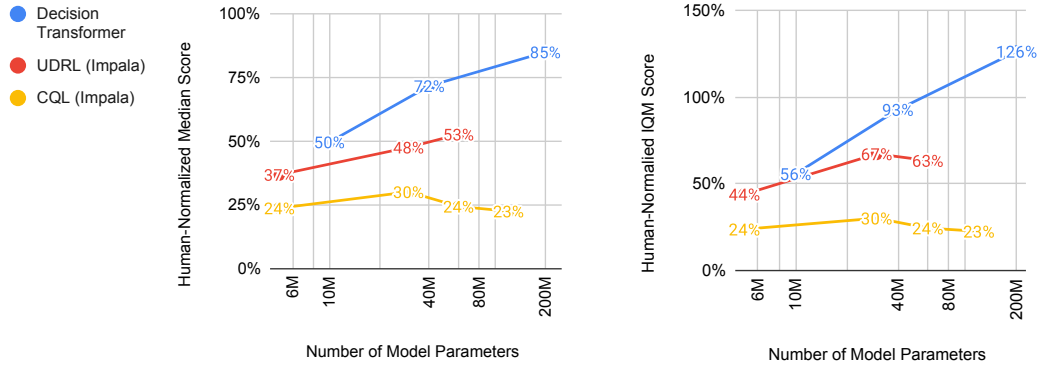

(a) Scaling of median scores for all training games with different model sizes and architectures.

(b) Scaling of IQM for all training games with different model sizes and architectures.

Figure 14: How UDRL (Impala architecture) performance scales with model size on training set games, in comparisons with Decision Transformer and CQL (Impala architecture).

Figure 14 shows clear advantages of Decision Transformer over UDRL with the Impala architecture. In the comparison between UDRL (Impala) and CQL that uses the same Impala network at each model size we evaluated, we observe that UDRL (Impala) outperforms CQL. The results show that the benefits of our method come not only from using network architectures, but also from the UDRL

formulation. Although it is not feasible to compare transformer with all possible convolutional architectures due to the broad design space, we believe these empirical results still show a clear trend favoring both UDRL and transformer architectures.

F Effect of Model Size on Training Speed

It is believed that large transformer-based language models train faster than smaller models, in the sense that they reach higher performance after observing a similar number of tokens [11, 4]. We find this trend to hold in our setting as well. Figure 15 shows an example of performance on two example games as multi-game training progresses. We see that larger models reach higher scores per number of training steps taken (thus tokens observed).

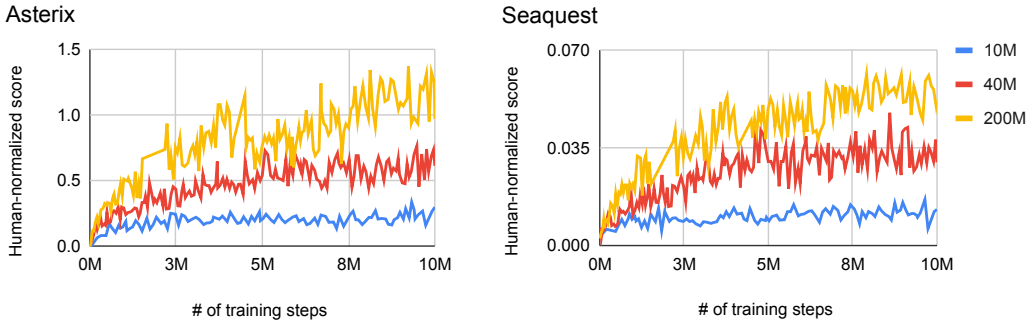

Figure 15: Example game scores for different model sizes as multi-game training progresses.

G Qualitative Attention Analysis

We find that the Decision Transformer model consistently attends to observation image patches that contain meaningful game entities. Figure 16 visualizes selected attention heads and layers for various games. We find heads consistently attend to entities such as player character, player's free movement space, non-player objects, and environment features.

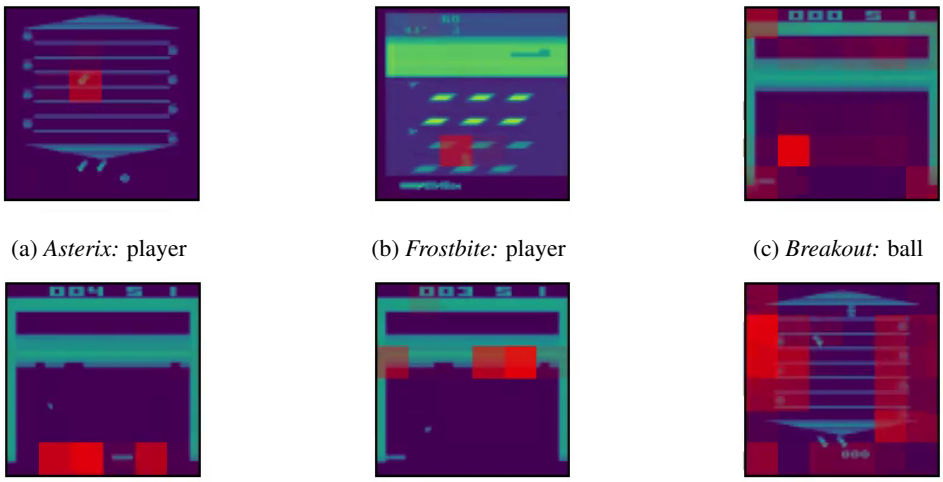

(a) *Asterix:* player (b) *Frostbite:* player (c) *Breakout:* ball

(d) *Breakout:* no paddle (e) *Breakout:* unbroken blocks (f) *Asterix:* non-players

Figure 16: Example image patches attended (red) for predicting next action by Decision Transformer.

H Raw Atari Scores

We report full raw scores of 41 training Atari games for best performing sizes of multi-game models in Table 2.

Game Name	DT (200M)	BC (200M)	Online DQN (10M)	CQL (60M)
Amidar	101.5	101.0	629.8	4.0
Assault	2,385.9	1,872.1	1,338.7	820.1
Asterix	14,706.3	5,162.5	2,949.1	950.0
Atlantis	3,105,342.3	4,237.5	976,030.4	16,800.0
BankHeist	5.0	63.1	1,069.6	20.0
BattleZone	17,687.5	9,250.0	26,235.2	5,000.0
BeamRider	8,560.5	4,948.4	1,524.8	3,246.4
Boxing	95.1	90.9	68.3	100.0
Breakout	290.6	185.6	32.6	62.0
Carnival	2,213.8	2,986.9	2,021.2	440.0
Centipede	2,463.0	2,262.8	4,848.0	2,904.0
ChopperCommand	4,268.8	1,800.0	951.4	400.0
CrazyClimber	126,018.8	123,350.0	146,362.5	139,300.0
DemonAttack	23,768.4	7,870.6	446.8	1,202.0
DoubleDunk	-10.6	-1.5	-156.2	-2.0
Enduro	1,092.6	793.2	896.3	729.0
FishingDerby	11.8	5.6	-152.3	18.4
Freeway	30.4	29.8	30.6	32.0
Frostbite	2,435.6	782.5	2,748.4	408.0
Gopher	9,935.0	3,496.3	3,205.6	700.0
Gravitar	59.4	12.5	492.5	0.0
Hero	20,408.8	13,850.0	26,568.8	14,040.0
IceHockey	-10.1	-8.3	-10.4	-10.5
Jamesbond	700.0	431.3	264.6	500.0
Kangaroo	12,700.0	12,143.8	7,997.1	6,700.0
Krull	8,685.6	8,058.8	8,221.4	7,170.0
KungFuMaster	15,562.5	4,362.5	29,383.1	13,700.0
NameThisGame	9,056.9	7,241.9	6,548.8	3,700.0
Phoenix	5,295.6	4,326.9	3,932.5	1,880.0
Pooyan	2,859.1	1,677.2	4,000.0	330.0
Qbert	13,734.4	11,276.6	4,226.5	11,700.0
Riverraid	14,755.6	9,816.3	7,306.6	3,810.0
RoadRunner	54,568.8	49,118.8	25,233.0	50,900.0
Robotank	63.2	44.6	9.2	17.0
Seaquest	5,173.8	1,175.6	1,415.2	643.0
TimePilot	2,743.8	1,312.5	-883.1	2,400.0
UpNDown	16,291.3	10,454.4	8,167.6	5,610.0
VideoPinball	1,007.7	1,140.8	85,351.0	0.0
WizardOfWor	187.5	443.8	975.9	500.0
YarsRevenge	28,897.9	20,738.9	18,889.5	19,505.4
Zaxxon	275.0	50.0	-0.1	0.0

Table 2: Raw scores of 41 training Atari games for best performing multi-game models.

References

[1] Rishabh Agarwal, Dale Schuurmans, and Mohammad Norouzi. An optimistic perspective on offline reinforcement learning. In *International Conference on Machine Learning*, pages 104–114. PMLR, 2020.

[2] Rishabh Agarwal, Max Schwarzer, Pablo Samuel Castro, Aaron C Courville, and Marc Bellemare. Deep reinforcement learning at the edge of the statistical precipice. *Advances in Neural Information Processing Systems*, 34, 2021.

[3] Marc G Bellemare, Will Dabney, and Rémi Munos. A distributional perspective on reinforcement learning. In *International Conference on Machine Learning*, pages 449–458. PMLR, 2017.

[4] Aakanksha Chowdhery, Sharan Narang, Jacob Devlin, Maarten Bosma, Gaurav Mishra, Adam Roberts, Paul Barham, Hyung Won Chung, Charles Sutton, Sebastian Gehrmann, et al. Palm: Scaling language modeling with pathways. *arXiv preprint arXiv:2204.02311*, 2022.

[5] Jacob Devlin, Ming-Wei Chang, Kenton Lee, and Kristina Toutanova. Bert: Pre-training of deep bidirectional transformers for language understanding. *arXiv preprint arXiv:1810.04805*, 2018.

[6] Alexey Dosovitskiy, Lucas Beyer, Alexander Kolesnikov, Dirk Weissenborn, Xiaohua Zhai, Thomas Unterthiner, Mostafa Dehghani, Matthias Minderer, Georg Heigold, Sylvain Gelly, et al. An image is worth 16x16 words: Transformers for image recognition at scale. *arXiv preprint arXiv:2010.11929*, 2020.

[7] Lasse Espeholt, Hubert Soyer, Remi Munos, Karen Simonyan, Vlad Mnih, Tom Ward, Yotam Doron, Vlad Firoiu, Tim Harley, Iain Dunning, et al. Impala: Scalable distributed deep-rl with importance weighted actor-learner architectures. In *International Conference on Machine Learning*, pages 1407–1416. PMLR, 2018.

[8] Scott Fujimoto, David Meger, and Doina Precup. Off-policy deep reinforcement learning without exploration. In *International Conference on Machine Learning*, pages 2052–2062. PMLR, 2019.

[9] Caglar Gulcehre, Ziyu Wang, Alexander Novikov, Thomas Paine, Sergio Gómez, Konrad Zolna, Rishabh Agarwal, Josh S Merel, Daniel J Mankowitz, Cosmin Paduraru, et al. Rl unplugged: A suite of benchmarks for offline reinforcement learning. *Advances in Neural Information Processing Systems*, 33:7248–7259, 2020.

[10] Ari Holtzman, Jan Buys, Li Du, Maxwell Forbes, and Yejin Choi. The curious case of neural text degeneration. *arXiv preprint arXiv:1904.09751*, 2019.

[11] Jared Kaplan, Sam McCandlish, Tom Henighan, Tom B Brown, Benjamin Chess, Rewon Child, Scott Gray, Alec Radford, Jeffrey Wu, and Dario Amodei. Scaling laws for neural language models. *arXiv preprint arXiv:2001.08361*, 2020.

[12] Volodymyr Mnih, Koray Kavukcuoglu, David Silver, Andrei A Rusu, Joel Veness, Marc G Bellemare, Alex Graves, Martin Riedmiller, Andreas K Fidjeland, Georg Ostrovski, et al. Human-level control through deep reinforcement learning. *nature*, 518(7540):529–533, 2015.

[13] Aaron van den Oord, Yazhe Li, and Oriol Vinyals. Representation learning with contrastive predictive coding. *arXiv preprint arXiv:1807.03748*, 2018.

[14] Juergen Schmidhuber. Reinforcement learning upside down: Don't predict rewards–just map them to actions. *arXiv preprint arXiv:1912.02875*, 2019.

[15] Rupesh Kumar Srivastava, Pranav Shyam, Filipe Mutz, Wojciech Jaśkowski, and Jürgen Schmidhuber. Training agents using upside-down reinforcement learning. *arXiv preprint arXiv:1912.02877*, 2019.

[16] Jianlin Su, Yu Lu, Shengfeng Pan, Bo Wen, and Yunfeng Liu. Roformer: Enhanced transformer with rotary position embedding. *arXiv preprint arXiv:2104.09864*, 2021.

[17] Ashish Vaswani, Noam Shazeer, Niki Parmar, Jakob Uszkoreit, Llion Jones, Aidan N Gomez, Łukasz Kaiser, and Illia Polosukhin. Attention is all you need. *Advances in neural information processing systems*, 30, 2017.

[18] Mengjiao Yang and Ofir Nachum. Representation matters: Offline pretraining for sequential decision making. In *International Conference on Machine Learning*, pages 11784–11794. PMLR, 2021.